The International Journal of Engineering and Science (IJES)
|| Volume || 14 || Issue 9 || September || Pages || PP 49-60 || 2025 ||
ISSN (e): 2319 – 1813 ISSN (p): 2319 – 1805

Behavior of rotating annular deformable rough plates under squeeze film conditions using the Rabinowitz Fluid Model (RFM)

Dr. Jatinkumar V. Adeshara
Vishwakarma Government Engineering College, Chandkheda, Ahmedabad – 382424.

Dr. Hardik P. Patel
Department of Humanity and Science, LJIET, L J K University. Ahmedabad.

Dr. Sureshkumar G. Sorathiya
Shreyarth University, Ahmedabad, Gujarat, India.
Prin. Dr. Ms. Pragna A. Vadher
Principal, Government Science College, Idar, India.

Dr. Gunamani Deheri
S. P. University, Vallabh Vidyanagar – 388 120, Gujarat State, India.
Rakesh M. Patel
Department of Mathematics, Gujarat Arts and Science College, Ahmedabad.
All the authors have contributed equally.
∗ Corresponding author

Date of Submission: 15-09-2025 Date of acceptance: 30-09-2025

Extended Abstract:
This article aims to understand how porosity and surface roughness influence the dynamics between two moving plates in hydrodynamic lubrication scenarios. A study has been analysed the effects of roughness and porous structures on annular rotating discs operating under squeeze film conditions. With making use of a Gaussian quadrature integral formula, the analysis discusses the characteristics of deformable roughness in relation to the equations of Rabinowitz fluid flow (RFF) through a small perturbation method (SPM). Further, how nonlinear parameters affect porosity, roughness impact on film pressure, load carrying capacity and the time required for squeezing in annular discs has also been discussed. Findings are presented in tabular as well as graphical form show a significant influence of porosity and deformable roughness on annular plates. Moreover, a notable enhanced performance observed when considering dilatant fluids with RFF over rough surfaces.

Keywords:

Rotating annular discs	Squeeze film pressure	Deformable rough surface
Porosity	Load bearing capacity	Porous structures

Subject classification could fall under:

- **Engineering / Mechanical Engineering**
  - Tribology (friction, lubrication, and wear)
  - Fluid Film Lubrication
  - Hydrodynamic / Hydrostatic Bearings
- **Applied Mathematics & Mechanics**
  - Nonlinear Fluid Dynamics
  - Non-Newtonian Fluid Models
  - Squeeze Film Theory
- **Physics**
  - Continuum Mechanics
  - Rheology of Non-Newtonian Fluids

Nomenclature and List of Symbols with Acronyms

Acronyms

RAN	Rotating Annular Disks
SFP	Squeeze Film Pressure
DRS	Deformable Rough Surface
LCC	Load Carrying Capacity
PS	Porous Structures
NF	Newtonian Fluids
NLRE	Non-Linear Reynolds Equation
NNF	Non-Newtonian Fluids
RFM	Rabinowitz Fluid Model
SRT	Squeeze Response Time

Geometrical Parameters

r1*, r2*	Inner / outer radius of annular disks [m]
Ω	Ratio of inner to outer radius, Ω = r1*/r2*
h0, h1	Inlet / outlet film thickness [m]
$\bar{h}$	Nominal film height [m]
$\hat{h}$, h*	Film thickness, $\hat{h} = \bar{h} + \bar{h}s$ and h* = $\hat{h}/\hat{h}0$ [m]
$\bar{h}s$	Film height deviation from nominal level [m]
c, c*	Greatest asperity variation; c* = c/$\hat{h}0$
θ	Circumferential coordinate [°]

Velocities and Coordinates

h•	Squeeze velocity = $-\partial h/\partial t$ [m/s]
$\hat{r}$, $\hat{z}$, r*	Coordinates of disks
û, ŵ	Velocity components in $\hat{r}$, $\hat{z}$ directions [m/s]
ûp, ŵp	Axial and radial velocity components in porous region [m/s]
ŵprs	Through-flow velocity on porous boundary [m/s]

Porous Structures

$\hat{H}0$, H0*	Porous pad thickness, H0* = φ$\hat{H}0/\hat{h}0$ [m]
$\acute{R}0$, R0*	Porous pad thickness, R0* = φ$\acute{R}0/\hat{h}0$ [m]
$\bar{p}$	Film pressure in porous region

Dimensionless Groups and Film Properties

p, P*	Squeeze film pressure, P* = (p$\hat{h}$0^3)/(μ0 r2^2 h•)
w, W*	Load carrying capacity, W* = (W$\hat{h}$0^3)/(μ0 r2^4 h•)
t, T*	Squeeze response time, T* = (W$\hat{h}$0^2 t)/(μ0 r2^4)

Material and Fluid Properties

$\hat{\mu}$	Dynamic viscosity of NNF [Pa·s]
$\tau\hat{r}\hat{z}$	Element of stress tensor [Pa]
$\hat{\psi}$	Permeability of porous region [m2]
$\hat{\mu}$	Coefficient of porosity [pu]
$\hat{\varphi}$	Dynamic viscosity of NNF [Pa·s]
ξ	Nonlinear factor (RFM) [–]

Surface Roughness Parameters

ξ	Random variable of surface roughness [–]
σ, σ*	Standard deviation of roughness / dimensionless
α, α*	Variance / dimensionless
ε, ε*	Skewness / dimensionless
δ, δ*	Deformation / dimensionless

I. Literature review and introduction:

Squeeze film (SF) is used in a variety of applications, such as turbo machinery, disc clutches, and viscous lock systems. Recently, there has been a significant increase in interest in this area. The performance of annular plates under SF has been studied under Newtonian fluids (NF) and non-Newtonian fluids (NNF) by Allen and McKillop [1], and Naduvinamani et al. [2]. It has been discovered that squeeze film (SF) increases the efficiency and reliability of bearings while also prolonging their lifespan. The NF is a broad term for the linear relationship between shear strain and the rate of change. Experimental research has shown that novel fluids can be constructed from an NF to include some additional components that behave as an NNF. Consist of high-molecular-weight polymers, viscosity index improvers, poly isobutylene, etc. (Spike [3]).

The non-Newtonian fluids (NNF) have a non-linear relationship with both the rate of shear strain and the shear stress. Different NNF models, such as the power law fluid model, Rabinowitz fluid model (RFM), and couple-stress fluid model, have been tested by a number of tribologists to investigate the performance of bearings. Lin and Hung [4] have investigated the performance of circular plates lubricated with a couple stress fluid models and a power-law fluid model by Wang et al. [5]. Several researchers have studied the demonstration of the RFM for different types of bearings. Wada and Hayashi [6, 7] were the first to study theoretically and experimentally the mechanism of journal bearing in the presence of pseudo plastic fluids. Furthermore, Lin [8] and Siddangouda et al. [9] investigated the performance of parallel annular discs and static characteristics of an inclined plane slider bearing under the condition of RFM.

These studies suggest that under RFM the bearing performance is influenced by the characteristics of the dilatant fluids, whereas the pseudo-plastic behaviour results in a lower concentration of bearing stability compared to NF. For five decades, permeable materials have been widely used in industry to improve bearing performance (Bujurke et al. [10], Morgan and Cameron [11]). With the use of Darcy's model, Morgan and Cameron [10] were the first researchers who investigated the porous effect on bearing surfaces. Patel et al. [12] have considered double-layer porous surface with a curved squeeze film. Bhat and Deheri [13] conducted a study on squeeze film behavior in porous annular discs that are lubricated with magnetic fluid.

Recently, Walicka et al. [14], Rao and Rahul [15– 17], and Rahul et al. [18] have applied the RFM on a curvilinear and SF bearing to study the characteristics of the dilatant fluid between the porous media. These researchers were concerned with how the porous wall affected the performance of the bearings. It was concluded that the Rabinowitz fluid property, which exists in porous media, has a substantial impact on the bearings' characteristics and lengthens their lifetime. The goal of many researchers is to show how SR affects the thin film lubrication bearing. The bearing performance, including pressure, load, friction, drags, and other factors, is influenced by this conditions surface roughness.

Various methodologies have been introduced to examine the impact of SR on the performance of bearings. Christensen [19, 20] first established the stochastic theory of thin film lubrication of rough bearing surfaces. The combined effects of SR and porosity with MHD between annular discs have been taken into consideration by Baksh and Naganagowda [21]. By analyzing the permeability influence on the rotor linear stability, D'Agostino et al. [22] examined the unstable oil film forces in porous bearings.Vashi et al. [23], have considered the Neuringer-Rosenzweig model to investigate the performance of circular stepped plates in the existence of couple stress, porosity, and SR Siddangouda et al. [24] investigated the combined impact of SR and viscosity change brought on by additives on long journal bearing.

According to Munshi et al. [25], a rough porous sine film slider bearing with Ferro fluid lubrication was subjected to a sinusoidal magnetic field. Shimpi and Deheri [26] investigated the deformation effect of a magnetic fluid-based squeeze film in rough rotating curved porous annular plates. Patel et al. [27] investigated the lubrication of a rough porous hyperbolic slider bearing with slip velocity using Ferro fluid. Patel and Deheri [28] studied the joint effect of slip velocity and roughness on the Ferro fluid lubrication of a curved rough annular squeeze film using the Jenkins model. Vashi et al. [29] studied the longitudinally rough porous circular stepping plates based on the Neuringer-Roseinweig (N R) model in the presence of couple stress. The influence of a porous structure, slip velocity, and Rosensweig's viscosity on the Ferro fluid-based squeeze film on porous curved annular plates was explored by Patel et al. [30].

Pressure generations in a rough conical bearing using non-Newtonian Rabinowitz fluid with variable viscosity have been investigated by Rao and Rahul [31]. A hydrostatic conical bearing that is externally pressured and lubricated with RFM has been studied by Walicka et al. [32] for how wall porosity and surface roughness affect steady performance. Recently, Rahul and Rao [33, 34] investigated the behavior of annular discs and circular stepping plates in the presence of a viscosity variable of Rabinowitz fluid with a rough and porous surface. A one-dimensional azimuthal (Radial) roughness pattern on the rough porous circular plate increases (decreases) the load-carrying capacity and the squeeze film time as compared to the corresponding smooth case has been discussed. Moreover, in circular stepped plates with the presence of the porous wall, the load capacity, and squeeze time decreases compared to non-porous case. Therefore, this study aims to investigate the behavior of a rotating annular bearing system under squeeze film conditions using the Rabinowitz Fluid Model (RFM).

Research gap:

The researchers concluded that transverse roughness patterns on the bearing surface can enhance both frictional power (FP) and life cycle cost (LCC). Despite the promising potential of squeeze film bearings, there remains a significant gap in research in this area. Most existing studies have not addressed the effects of porous discs, the Rabinowitz fluid model, or surface roughness, as noted in the literature review. Several key issues remain unexplored:

Analyzing the squeeze film characteristics in annular discs using the Rabinowitz fluid model to assess the impact of porosity and surface roughness. Investigating how parameters ω, H_0^* R_0^* and c^* influence the trend of $P^*$for a constant Ω. additionally, determining the effects of these parameters on the trend of W^* for a constant h^* and Ω.Examining the impact of ω, H_0^* R_0^* and c^* on t^* for a constant h^* and Ω and evaluating the performance of the disc across various values of ω and Ω.Notably, the study by Lin [8] does not address the following points: Applying stochastic processes to analyze surface roughness (SR) in annular discs. This would involve creating two hydrodynamic lubrication models: one for 1-D azimuthal roughness and another for 1-D radial roughness.Proposing two-part geometry for disc coatings, where the first part—known as the nominal film thickness—includes long-wavelength disturbances, while the second part accounts for SR that varies randomly from this nominal level.

Utilizing, Christensen's stochastic theory to derive an averaged, non-linear modified Reynolds equation.Employing probability density functions, expectations, averages, and variances to analyze the effects of c^* on P^*, W^* and t^*.The exploration of porous surfaces with specific roughness effects on annular discs represents a novel and intriguing research area, with significant implications for various applications. This research aims to investigate the combined effects of surface porosity and roughness in annular discs, marking a new frontier in engineering and materials science.

Novelty:

Exploring the interplay between surface porosity and roughness in annular discs represents a compelling area of research. By integrating both features, researchers can create materials and structures with unique properties and capabilities that cannot be achieved by studying them in isolation. For instance, incorporating porous and rough surfaces into circular discs can significantly enhance heat transfer efficiency, which has promising applications in heat exchangers where improved thermal performance can lead to energy savings.

Understanding how the interaction between porosity and roughness influences fluid flow within annular discs is particularly innovative. The insights gained from this research could be invaluable for designing fluidic devices, pumps, and turbines. Furthermore, developing novel surface modification techniques to create specific porous and rough structures in annular discs could benefit specialized applications such as biomedical devices, aircraft components, and filtration systems.

Objective:

One of the primary objectives is to optimize the design of porous and rough annular discs for specific applications. Researchers can concentrate on improving heat transfer efficiency, minimizing pressure drop, or enhancing filtration performance based on the particular requirements of each application.

This involves creating analytical models to predict how different combinations of porosity and roughness affect fluid flow patterns and structural integrity within the annular discs. Ultimately, the research seeks to refine the design, enhance our understanding of behavior and explore the applications of annular discs with integrated porous and rough surfaces to meet the distinct needs of various industries and technologies.

Problem formulation and mathematical solutions:

Squeeze film formed by two permeable ring-shaped discs with internal and external radii r_1^* and r_2^* stirring toward one another at a squash velocity ($-\partial h/\partial t$), is shown in Figure (A). Porous media with thickness H_0 and capillary radii R_0 are present in the upper disc.The RFM is also known as the non-linear cubic power that correlates the shear stress τ_{rz} and strain rate ($\partial u/\partial z$). It is described mathematically as

$$\tau_{rz} = \mu \frac{\partial u}{\partial z} - \xi \tau^3{}_{rz} \quad (1)$$

where μ is the dynamic viscosity of the NNF. The non-linear component ξ, which defines the feature of RFM, can be used to discriminate between three different types of fluids.

Fluids are referred to as pseudo-plastic if $\xi > 0$

Fluids are referred to as Newtonian if $\xi = 0$

Fluids are referred to as dilatant if $\xi < 0$

The following continuity and momentum equations have been used to govern the governing equations for the RFM (Lin [8]; Rahul et al. [14,15]).

$$\frac{1}{r}\frac{\partial (ru)}{\partial r} + \frac{\partial w}{\partial z} = 0 \quad (2)$$

$$\frac{1}{r}\frac{\partial p}{\partial r} - \frac{\partial \tau_{rz}}{\partial z} = 0 \quad (3)$$

$$\frac{\partial p}{\partial z} = 0 \quad (4)$$

Rough porous annular disc boundary conditions are described by Equations (5) and (6).

Upper surface:

$z = 0$; $u(r, 0, t) = 0$, $w(r, 0, t) = w_{prs}$ (5)

Lower surface:

$z = h$; $u(r, h, t) = 0$, $w(r, h, t) = -\partial h/\partial t$ (6)

where u(r, h, t) and w(r, h, t) are the components of velocity in r and z directions, respectively. w_{prs} is the velocity of a through-flow on the upper boundary of the porous layer. The velocity component u is determined by substituting Equation 1 by the above Equation (3) and integrating while taking boundary conditions Equations (5) and (6) into consideration.

$$u(r,z) = \frac{1}{2\mu}\left[G^0(h,z)\frac{\partial p}{\partial r} + \zeta\left(\frac{\partial p}{\partial r}\right)^3 G^1(h,z)\right] \quad (7)$$

By substituting Equation 7 into Equation 2 and integrating with respect to z, one can obtain:

$$\frac{1}{r}\frac{\partial}{\partial r}\left[r\int_{z=0}^{z=h}\frac{1}{2h}\left(G^0(h,z)\frac{\partial p}{\partial r} + \zeta G^1(h,z)\left(\frac{\partial p}{\partial r}\right)^3\right)dz\right] = -\int_{z=0}^{z=h}\frac{\partial w}{\partial z}dz \quad (8)$$

The modified NLRE for the rough porous annular discs is given by applying the boundary conditions (5) and (6) into Equation 8 as follows:

$$\frac{1}{r}\frac{\partial}{\partial r}\left[rG(h)\left\{\left(\frac{\partial p}{\partial r}\right) + \frac{3}{20}\chi[G(h)]^{2/3}\left(\frac{\partial p}{\partial r}\right)^3\right\}\right] = 12\mu\left[\frac{\partial h}{\partial t} - w_{prs}\right] \quad (9)$$

Let the non-Newtonian fluid flow within the porous layer adhere to the modified Darcy's law, assuming the layer is isotropic and homogeneously distributed. The capillary network that constitutes these homogeneous, isotropic porous layers has an average radius of R_0 and a porosity of ψ. The axial and radial components of the velocity through the porous wall are transformed as follows:

$$u_p = \frac{\psi}{\mu}\left(-\frac{\partial p}{\partial r}\right) + \frac{\psi}{\mu}\frac{\zeta R_0^2}{6}\left(-\frac{\partial p}{\partial r}\right)^3 \quad (10)$$

$$w_p = \frac{\psi}{\mu}\left(-\frac{\partial p}{\partial z}\right) + \frac{\psi}{\mu}\frac{\zeta R_0^2}{6}\left(-\frac{\partial p}{\partial z}\right)^3 \quad (11)$$

Let ϕ represent the coefficient of porosity, while u_p and $\psi = \frac{\varphi {R_0}^2}{8}$ denote the velocity components and the permeability of the porous layer, respectively. For porous fluids, the cross-velocity component w_{prs} is always continuous and is equal to

$$(w_p)_{\text{at } z=0} = (w_{prs})_{\text{at } z=0} \quad (12)$$

Substituting Equation12 into Equation9, the result obtained is known as the modified NLRE which is expressed as:

$$\frac{1}{r}\frac{\partial}{\partial r}\left[rh^3\left\{\left(\frac{\partial p}{\partial r}\right) + \frac{3}{20}\zeta h^2\left(\frac{\partial p}{\partial r}\right)^3\right\}\right] = 12\mu\left[\frac{\partial h}{\partial t} - \frac{\psi}{\mu}\left(-\frac{\partial p}{\partial z}\right) + \frac{\zeta {R_0}^2}{6}\left(-\frac{\partial p}{\partial z}\right)^3\right]_{z=0} \quad (13)$$

The modified version of Darcy's law satisfied Equation 2 for the porous layer (Walickaetal. [13], Rao and Rahul [14,15])

$$\frac{1}{r^*}\frac{\partial\left(r^* {u_p}^*\right)}{\partial r^*} + \frac{\partial {w_p}^*}{\partial z^*} = 0 \quad (14)$$

By substituting Equation 10 and Equation 11 into Equation14 we obtain

$$\frac{\partial}{\partial z^*}\left[\left(-\frac{\partial p^*}{\partial z^*}\right) + \frac{\chi {R_0}^{*2}}{6}\left(-\frac{\partial p^*}{\partial z^*}\right)^3\right] = -\frac{1}{r^*}\frac{\partial}{\partial r^*}\left[r^*\left\{\left(-\frac{\partial p^*}{\partial r^*}\right)\right\} + \frac{\chi {R_0}^{*2}}{6}\left(-\frac{\partial p^*}{\partial r^*}\right)^3\right] \quad (15)$$

Integrating Equation15 with respect to z over the porous layer region [−ˆ H0,0],

$$\left[\left(-\frac{\partial p^*}{\partial z^*}\right) + \frac{\chi {R_0}^{*2}}{6}\left(-\frac{\partial p^*}{\partial z^*}\right)^3\right] = -\frac{1}{r^*}\frac{\partial}{\partial r^*}\int_{-H_0^{*2}}^{0}\left[\left\{\left(-\frac{\partial p^*}{\partial r^*}\right)\right\} + \frac{\chi {R_0}^{*2}}{6}\left(-\frac{\partial p^*}{\partial r^*}\right)^3\right]dz^* \quad (16)$$

since

$$\left[\left(-\frac{\partial p^*}{\partial z^*}\right) + \frac{\chi {R_0}^{*2}}{6}\left(-\frac{\partial p^*}{\partial z^*}\right)^3\right]_{z^*=-H_0^*} = 0 \quad (17)$$

Using the Morgan-Cameron approximation [11], the Equation 18 is used in Equation 13, the modified NLRE, which is defined as

$$\frac{1}{r^*}\frac{\partial}{\partial r^*}\left[r^*\left\{f_1\left(h^*,\phi^*,{R_0}^*,{H_0}^*\right)\frac{\partial p^*}{\partial r^*} + 0.15\chi f_2\left(h^*,\phi^*,{R_0}^*,{H_0}^*\right)\left(\frac{\partial p^*}{\partial r^*}\right)^3\right\}\right] = 12\mu^*\left(\frac{\partial h^*}{\partial t^*}\right) \quad (18)$$

where

$$f_1\left(h^*,\phi^*,R_0{}^*,H_0{}^*\right)=g(h)-0(1.5)\phi^* R_0{}^{*2}H_0{}^*$$
$$f_2\left(h^*,\phi^*,R_0{}^*,H_0{}^*\right)=\left[g(h)^{1/5}\right]+(1.66)\phi^* R_0{}^{*4}H_0{}^*$$

Surface roughness:

In the case of surface roughness the concept to film thickness is divided into two parts.

$h^* = h(r^*)+ h_s^*(r^*,\theta,\xi)$, (19)

where $h(r^*)$ represents the apparent smooth part of the film geometry, $h_s^*=\delta_1+\delta_2$ provides the arbitrary region resulting from SR irregularities measured from the apparent level and ξ represents their regular variable that represents the apparent positive definite roughness arrangement. The Gaussian distribution is used to calculate the roughness profile heights that are valid upto three standard deviations or more for a range of lubricated rough surfaces. A likelihood rough distribution function is defined by Christensen and Tonder:

$$f(h_s{}^*)=1.093c^{-7}\left(c^2-h_s{}^*\right)^3;-c\le h_s{}^*\le c \quad (20)$$

where c denotes the maximum deviation from the mean film thickness, i.e., c = ±3σ, where σ is the standard deviation. Using expected values in Equation 20, we obtain the following equation of the averaged NLRE

$$\frac{1}{r^*}\frac{\partial}{\partial r^*}\left[r^*\left(E\left\{f_1\left(h^*,\phi^*,R_0{}^*,H_0{}^*\right)\right\}\frac{\partial E(p)}{\partial r^*}\right)+0.15\chi\left(E\left\{f_2\left(h^*,\phi^*,R_0{}^*,H_0{}^*\right)\right\}\left(\frac{\partial E(p)}{\partial r^*}\right)^3\right)\right]=12\mu^*\frac{\partial E(h^*)}{\partial t^*} \quad (21)$$

The expectation operator E(·) is expressed as follows:

$$E(.)=\int_{-c}^{c} f(h_s{}^*)dh_s{}^* \quad (22)$$

By using stochastic theory, Christensen [16] has proposed two different types of 1-D roughness patterns: azimuthal and radial patterns. The patterns of roughness are confined edges and valleys flowing in the same direction. The film thickness region for the one-dimensional radial and azimuthal roughness is represented as follows:

$h^* = h^*(r^*) + h^*_s(\theta, \xi)$, radial roughness

$h^* = h^*(r^*) + h^*_s(r^*, \xi)$, azimuthally roughness. (23)

$$\frac{1}{r^*}\frac{\partial}{\partial r^*}\left[r^*\left(E\left\{G_1\left(h^*,\phi^*,R_0{}^*,H_0{}^*\right)\right\}\frac{\partial E(p)}{\partial r^*}\right)+0.15\chi\left(E\left\{G_2\left(h^*,\phi^*,R_0{}^*,H_0{}^*\right)\right\}\left(\frac{\partial E(p)}{\partial r^*}\right)^3\right)\right]=12\mu^*\frac{\partial E(h^*)}{\partial t^*} \quad (24)$$

$$G_1\left(h^*,\phi^*,R_0{}^*,H_0{}^*,c\right)=E\left\{f_1\left(h^*,\phi^*,R_0{}^*,H_0{}^*\right)\right\}\text{; radial roughness}$$
$$G_1\left(h^*,\phi^*,R_0{}^*,H_0{}^*,c\right)=\left[E\left\{1/f_1\left(h^*,\phi^*,R_0{}^*,H_0{}^*\right)\right\}\right]^{-1}\text{ azimuthal roughness}$$
$$G_2\left(h^*,\phi^*,R_0{}^*,H_0{}^*,c\right)=E\left\{f_2\left(h^*,\phi^*,R_0{}^*,H_0{}^*\right)\right\}\text{; radial roughness}$$
$$G_2\left(h^*,\phi^*,R_0{}^*,H_0{}^*,c\right)=\left[E\left\{1/f_2\left(h^*,\phi^*,R_0{}^*,H_0{}^*\right)\right\}\right]^{-1}\text{ azimuthal roughness} \quad (25)$$

Currently, the problem is minimizing the constructing methods for estimating the left side of Equation 24 according to a specified roughness pattern. The measurement of mean FP involves the evaluation of the standard estimate of distinct film thicknesses. The probability density function is incorporated by Equation 20. The accompanying expected estimations of film thickness is discussed in the work by Walicka et al. [23]. The predicted values of film thickness feature E(hˆ = i) ,i = 1, 2, . . . , 6, are not suitable for numericalpurposes for small Δ values, as there are variations when small amounts are involved, resulting in a loss in large digits. Hence, expansions of Taylor's powers Δ are proposed. The expansion of these film thickness functions in series

The pressure boundary conditions for the NLRE are given by Equation 26

$p^ = 0$ at $r^ = 1$, $p^ = 0$ at $r^ = 1$. (26)

Introducing the dimensionless variables and parameters

$$r^* = \frac{\hat{r}}{\hat{r}_2}, \quad h^* = \frac{\hat{h}}{\hat{h}_0}, \quad H^* = \frac{\hat{H}}{\hat{h}_0}, \quad R^* = \frac{\hat{R}}{\hat{h}_0},$$
$$\Omega = \frac{\hat{r}_1}{\hat{r}_2}, \quad c^* = \frac{c}{\hat{h}_0}, \tag{31}$$

$$P^* = \frac{p\hat{h}_0^{\,3}}{\hat{\mu}_0\hat{r}_2^2(-d\hat{h}/d\hat{t})}, \quad \omega = \frac{\varkappa\hat{\mu}_0^2\hat{r}_2^2(-d\hat{h}/d\hat{t})}{\hat{h}_0^4}.$$

Under the above mentioned dimensionless variables and parameters, the NLRE Equation 25 is expressed as:

$$\frac{\partial}{\partial r^*}\left[r^* G_1^*(h^*, R_0^*, H_0^*, c^*)\left(\frac{\partial P^*}{\partial r^*}\right)\right.$$
$$\left.+\frac{3}{20}\omega G_2^*(h^*, R_0^*, H_0^*, c^*)\left(\frac{\partial P^*}{\partial r^*}\right)^3\right] = -12r^*, \tag{32}$$

where

$$G_1(h^*, R^*, H^*, c^*) =$$
$$\begin{cases} E\{f_1(h^*, R_0^*, H_0^*)\}, & \text{radial roughness} \\ [E\{1/f_1^*(h^*, R_0^*, H_0^*)\}]^{-1}, & \text{azimuthal roughness} \end{cases} \tag{33}$$

$$G_2(h^*, R^*, H^*, c^*) =$$

$$\begin{cases} E\{f_2(h^*, R_0^*, H_0^*)\}, & \text{radial roughness} \\ \left[E\left\{1/f_2^*(h^*, R_0^*, H_0^*)\right\}\right]^{-1}, & \text{azimuthal roughness} \end{cases} \quad (34)$$

where ω represents the non-dimensional non-linear factor that specifies the RF behaviour. If, ω = 0 the fluids will behave like NF; ω > 0, the fluids will decompose as pseudoplastic fluids and ω < 0, the fluids will be dilatant fluids. The boundary condition in terms of dimensionless form is:

$$P^* = 0 \text{ at } r^* = \Omega, P^* = 0 \text{ at } r^* = 1 \quad (35)$$

The value of the pseudoplastic coefficient κ depends on the type and quantity of additives which can be determined experimentally [7]. Thus, the values of ω can be calculated with the appropriate value of κ. However, for the validity of the present analysis, the value of ω is restricted to $|\omega| < 0.01$. It is discovered that the dimensionless non-Newtonian averaged modified NLRE is nonlinear in terms of P^*. A small perturbation method based on Lin [8], Rahul and Rao [14, 15, 24] is used to get approximate analytical solutions. Therefore, the classical perturbation method is used to solve it. The perturbation series for P can be expressed in the form:

$$P^* = P^*_0 + \omega P^*_1 + \omega^2 P^*_2 + \ldots \quad (36)$$

For $\omega \ll 1$, it is sufficient, for the analysis, to consider the first order term in ω as follows: For small values of the nonlinear parameter ω, the FP is perturbed:

$$P^* = P^*_0 + \omega P^*_1 \quad (37)$$

For the higher values of ω, second and higher-order terms can be considered to increase the accuracy of the results. However, for the higher values of ω, it is more appropriate to adopt a numerical solution procedure such as the finite element method to solve the Reynolds equation. To obtain the FP P^*_0 and P^*_1, we substitute Equation 37 into the modified NLRE Equation 32

$$\frac{\partial}{\partial r^*}\left[r^* G_1^*(h^*, R_0^*, H_0^*, c^*)\left(\frac{\partial P^*}{\partial r^*}\right)\right] + 12r^* = 0, \quad (38)$$

$$\begin{aligned} &\frac{\partial}{\partial r^*}\left[r^* G_1^*(h^*, R_0^*, H_0^*, c^*)\left(\frac{\partial P^*}{\partial r^*}\right)\right] \\ &= -\frac{3}{20} G_2^*(h^*, R_0^*, H_0^*, c^*)\frac{\partial}{\partial r^*}\left[r\left(\frac{\partial P_0^*}{\partial r^*}\right)^3\right]. \end{aligned} \quad (39)$$

After solving Equation 38 and Equation 39, the perturbed dimensionless film pressures P^*_0 and $P^*_1$are:

$$P_0^* = \frac{3}{G_1^*(h^*, R_0^*, H_0^*, c^*)} \left[1 - r^{*2} + \left(\frac{\Omega^2 - 1}{\log \Omega}\right) \log r^*\right], \tag{40}$$

$$P_1^* = -\frac{A_4}{G_1^*(h^*, R_0^*, H_0^*, c^*)} \log r^* - \frac{3}{20} \frac{G_2^*(h^*, R_0^*, H_0^*, c^*)}{G_1^*(h^*, R_0^*, H_0^*, c^*)} \left\{ \left[54(1 - r^{*4}) - 54A_4(1 - r^{*2}) - 18A_4^2 \log r^*\right] + \frac{1}{2} A_4^3 \left(\frac{1}{r^{*2}} - 1\right) \right\}, \tag{41}$$

where

$$A_4 = -\frac{3(1 - \Omega^2)}{\log \Omega}$$

$$A_2 = \frac{3}{20} \frac{G_2^*(h^*, R_0^*, H_0^*, c^*)}{G_1^{*4}(h^*, R_0^*, H_0^*, c^*)} \tag{42}$$

$$\frac{1}{\log \Omega} \left\{ 54(1 - r^{*4}) - 54A_4(1 - \Omega^2) - 18A_4^2 \log S + \frac{1}{2} A_4^3 \left(\frac{1}{\Omega^2} - 1\right) \right\}.$$

The FP is integrated into the domain [r^1, r^2] to get the LCC of annular discs.

$$W = 2\pi \int_{\hat{r}_1}^{\hat{r}_2} p\hat{r}d\hat{r}. \qquad (43)$$

The dimensionless form of Equation 43 is given below:

$$W^* = \frac{\hat{W}\hat{h}_0^3}{\hat{\mu}_0\hat{r}_2^4(-d\hat{h}/dt)} = 2\pi \int_{\Omega}^{1} P^* r^* dr^*. \qquad (44)$$

Introducing the dimensionless SRT as:

$$t^* = \frac{W\hat{h}_0^2}{\hat{\mu}_0\hat{r}_2^4}\hat{t}, \qquad (45)$$

Introducing the dimensionless SRT as:

t∗ = Whˆ2 0 μˆ0rˆ 4 2 t,ˆ (45)

Substituting Equation 45 into Equation 44 yields the ordinary differential equation that incorporates the film height, which varies with SRT.

dh*/dt* = − 1 / W*. (46)

Future research:

In conclusion, the study of porous roughness annular discs is an important are of research with several applications in fluid dynamics, materials science, and engineering. Several promising directions stand out as having high potential for future research in this area, including advanced materials and fabrication modeling, and simulation, applications in energy and environmental engineering, surface modification techniques, data-driven approaches, etc. One can learn much more about porous roughness annular discs and unlock their potential to solve challenging problems across a range of industries by incorporating these research directions. Researchers can help make future engineering solutions more effective and sustainable by improving their design, performance, and applications.

Declarations:

Funding: The authors received no financial support for the research, authorship, or publication of this article.

Author Contributions: All authors contributed equally to this work.

Conflict of Interest: The authors declare no conflicts of interest.

Data Availability Statement: The data used in this study were obtained from publicly available online sources.

Institutional Review Board Statement: Not applicable.

Informed Consent Statement: Not applicable.

Ethics Statement: This manuscript does not involve any ethical concerns.

Disclosure of AI Use: Artificial intelligence (AI) tools (e.g., ChatGPT) were used to a limited extent, solely for language refinement and formatting assistance.

Citations and References:

[1]. C. Allen, A. McKillop. An investigation of the squeeze film between rotating annuli. ASME Journal of Lubrication Technology 92(3):435–441, 1970.

[2]. N. Naduvinamani, A. Siddangouda, A. Kadadi, S. Biradar. Effect of pressure dependent viscosity on squeeze film characteristics of micropolar fluid in convex curved plates. Tribology-Materials, Surfaces & Interfaces 9(3):154–158, 2015. https://doi.org/10.1080/17515831.2015.1107239

[3]. H. Spikes. The behaviour of lubricants in contacts: current understanding and future possibilities. Proceedings of the Institution of Mechanical Engineers, Part J: Journal of Engineering Tribology 208(1):3–15, 1994. https://doi.org/10.1243/PIME_PROC_1994_208_345_02

[4]. J. Lin, C. Hung. Combined effects of non-Newtonian rheology and rotational inertia on the squeeze film characteristics of parallel circular discs. Proceedings of the Institution of Mechanical Engineers, Part J: Journal of Engineering Tribology 222(4):629–636, 2008. https://doi.org/10.1243/13506501JET39

[5]. Y. Wang, J. H. Wu, L. Xu. Influence of power-law fluid on transient performance of liquid film seal based on the time-dependent non-Newtonian dynamic reynolds equation. Tribology International 159:106984, 2021. https://doi.org/10.1016/j.triboint.2021.106984

[6]. S. Wada, H. Hayashi. Hydrodynamic lubrication of journal bearings by pseudo-plastic lubricants: part 1, theoretical studies. Bulletin of JSME 14(69):268–278, 1971. https://doi.org/10.1299/jsme1958.14.268

[7]. S. Wada, H. Hayashi. Hydrodynamic lubrication of journal bearings by pseudo-plastic lubricants: part 2, experimental studies. Bulletin of JSME 14(69):279–286, 1971. https://doi.org/10.1299/jsme1958.14.279

[8]. J.-R. Lin. non-Newtonian squeeze film characteristics between parallel annular disks: Rabinowitz fluid model. Tribology international 52:190–194, 2012. https://doi.org/10.1016/j.triboint.2012.02.017A

[9]. Siddangouda, N. Naduvinamani, S. Siddapur. Effect of surface roughness on the static characteristics of inclined plane slider bearing: Rabinowitz fluid model. Tribology-Materials, Surfaces & Interfaces 11(3):125–135, 2017. https://doi.org/10.1080/17515831.2017.1347745

[10]. N. Bujurke, M. Jagadeeswar, P. Hiremath. Analysis of normal stress effects in a squeeze film porous bearing. Wear 116(2):237–248, 1987. https://doi.org/10.1016/0043-1648(87)90236-5

[11]. V. Morgan, A. Cameron. Mechanism of lubrication in porous metal bearings. In International Proceeding Conference Lubrication and Wear, Institute of Mechanical Engineering, vol. 89, pp. 151–157. Inst. Mech. Eng London, 1957.

[12]. N. C. Patel, J. R. Patel, G. M. Deheri. A comparative study of ferrofluid lubrication on double-layer porous squeeze curved annular plates with slip velocity. ActaPolytechnica 62(4):488–497, 2022. https://doi.org/10.14311/AP.2022.62.0488

[13]. M. Bhat, G. Deberi. Squeeze film behaviour in porous annular discs lubricated with magnetic fluid. Wear 151(1):123–128, 1991. https://doi.org/10.1016/0043-1648(91)90352-U

[14]. Walicka, E. Walicki, P. Jurczak, J. Falicki. Curvilinear squeeze film bearing with rough surfaces lubricated by a Rabinowitz–Rotem–Shinnar fluid. Applied Mathematical Modelling 40(17-18):7916–7927, 2016. https://doi.org/10.1016/j.apm.2016.03.048

[15]. P. Rao, A. Rahul, S. Agarwal. Effect of non-Newtonian lubrication of squeeze film conical bearing with the porous wall operating with Rabinowitz fluid model. Proceedings of the Institution of Mechanical Engineers, Part J: Journal of Engineering Tribology 232(10):1293–1303, 2018. https://doi.org/10.1177/1350650117749735

[16]. P. Rao, A. Rahul. Combined effect of viscosity variation and non-Newtonian Rabinowitz fluid in wide parallel rectangular-porous plate with squeeze-film characteristics. Meccanica 54(15):2399–2409, 2019. https://doi.org/10.1007/s11012-019-01092-2

[17]. P. S. Rao, A. Kumar Rahul. Effect of viscosity variation on non-Newtonian lubrication of squeeze film conical bearing having porous wall operating with Rabinowitz fluid model. Proceedings of the Institution of Mechanical Engineers, Part C: Journal of Mechanical Engineering Science 233(7):2538–2551, 2019. https://doi.org/10.1177/0954406218790

[18]. K. Rahul, M. K. Singh, S. Saha. Squeeze film lubrication analysis and optimization of porous annular disk with viscosity variation of non-Newtonian fluid: Rabinowitz fluid model. Tribology International 179:108060, 2023. https://doi.org/10.1016/j.triboint.2022.108060

[19]. H. Christensen. Stochastic models for hydrodynamic lubrication of rough surfaces. Proceedings of the institution of mechanical engineers 184(1):1013–1026, 1969. https: //doi.org/10.1243/PIME_PROC_1969_184_074_02

[20]. H. Christensen. Some aspects of the functional influence of surface roughness in lubrication. Wear 17(2):149–162, 1971. https://doi.org/10.1016/0043-1648(71)90025-1

[21]. S. AllaBaksh, H. BannihalliNaganagowda. Study of surface roughness with MHD and couple stress fluid on porous curved annular plates 62(6):574–588, 2022. https://doi.org/10.14311/AP.2022.62.0574

[22]. V. D'Agostino, A. Ruggiero, A. Senatore. Unsteady oil film forces in porous bearings: analysis of permeability effect on the rotor linear stability. Meccanica 44(2):207–214, 2009. https://doi.org/10.1007/s11012-008-9180-0

[23]. Y. D. Vashi, R. M. Patel, G. B. Deheri. Neuringer-Roseinweig model based longitudinally rough porous circular stepped plates in the existence of couple stress. ActaPolytechnica 60(3):259–267, 2020. https://doi.org/10.14311/AP.2020.60.0259

[24]. Siddangouda, T. Biradar, N. Naduvinamani. Combined effects of surface roughness and viscosity variation due to additives on long journal bearing. Tribology-Materials, Surfaces & Interfaces 7(1):21–35, 2013. https://doi.org/10.1179/1751584X13Y.0000000024

[25]. M. M. Munshi, A. R. Patel, G. B. Deheri. A study of ferrofluid lubrication based rough sine film slider bearing with assorted porous structure. ActaPolytechnica 59(2):144–152, 2019. https://doi.org/10.14311/AP.2019.59.0144

[26]. M. Shimpi, G. Deheri. Magnetic fluid based squeeze f ilm in rough rotating curved porous annular plates: Deformation effect. International Journal of Mathematical and Computational Sciences 7(8):1370 1380, 2013. https://doi.org/10.1155/2012/148281

[27]. S. Patel, G. Deheri, J. Patel. Ferro fluid lubrication of a rough porous hyperbolic slider bearing with slip velocity. Tribology in Industry 36(3):259–268, 2014.

[28]. J. Patel, G. Deheri. Combined effect of slip velocity and roughness on the Jenkins model based ferro fluid lubrication of a curved rough annular squeeze film. Journal of Applied Fluid Mechanics 9(2):855–865, 2016. https: //doi.org/10.18869/acadpub.jafm.68.225.24447

[29]. Y. D. Vashi, R. M. Patel, G. B. Deheri. Neuringer-Roseinweig model based longitudinally rough porous circular stepped plates in the existence of couple stress. ActaPolytechnica 60(3):259–267, 2020. https://doi.org/10.14311/AP.2020.60.0259

[30]. N. C. Patel, J. R. Patel, G. Deheri. An effect of a porous structure, slip velocity and Rosensweig's viscosity on the ferrofluid based squeeze film in porous curved annular plates. Journal of Nanofluids 12(2):498 505, 2023. https://doi.org/10.1166/jon.2023.1906

[31]. P. S. Rao, A. K. Rahul. Pressure generation in rough conical bearing using non-Newtonian Rabinowitsch fluid with variable viscosity. Industrial Lubrication and Tribology 71(3):357–365, 2019. https://doi.org/10.1108/ILT-01-2018-0035

[32]. Walicka, E. Walicki, P. Jurczak, J. Falicki. Influence of wall porosity and surfaces roughness on the steady performance of an externally pressurized hydrostatic conical bearing lubricated by a Rabinowitsch fluid. International Journal of Applied Mechanics and Engineering 22(3):717–737, 2017. https://doi.org/10.1515/ijame-2017-0045

[33]. K. Rahul, P. S. Rao. Rabinowitsch fluid flow with viscosity variation: application of porous rough circular stepped plates. Tribology International 154:106635, 2021. https://doi.org/10.1016/j.triboint.2020.106635

[34]. K. Rahul, M. K. Singh, S. Paul, et al. Performance analysis of annular disks with non-Newtonian Rabinowitsch fluid model: Influence of squeeze film pressure, surface roughness, porosity and viscosity variation. International Journal of Modern Physics B p. 2450268, 2023. [Online Ready]. https://doi.org/10.1142/S0217979224502680

[35]. Amit Kumar Rahula, Manoj Kumar Singha, Ravi Tiwarib, SourabhPaulb, PentyalaSrinivasaRaoc, RohahnBiswasd, SEMI-ANALYTICAL APPROACH-BASED STUDIES OF THE SQUEEZE FILM LUBRICATION BETWEEN ROUGH POROUS ANNULAR DISCS: RABINOWITSCH FLUID MODEL, ActaPolytechnica 63(6):439–450, 2023 https://doi.org/10.14311/AP.2023.63.0439

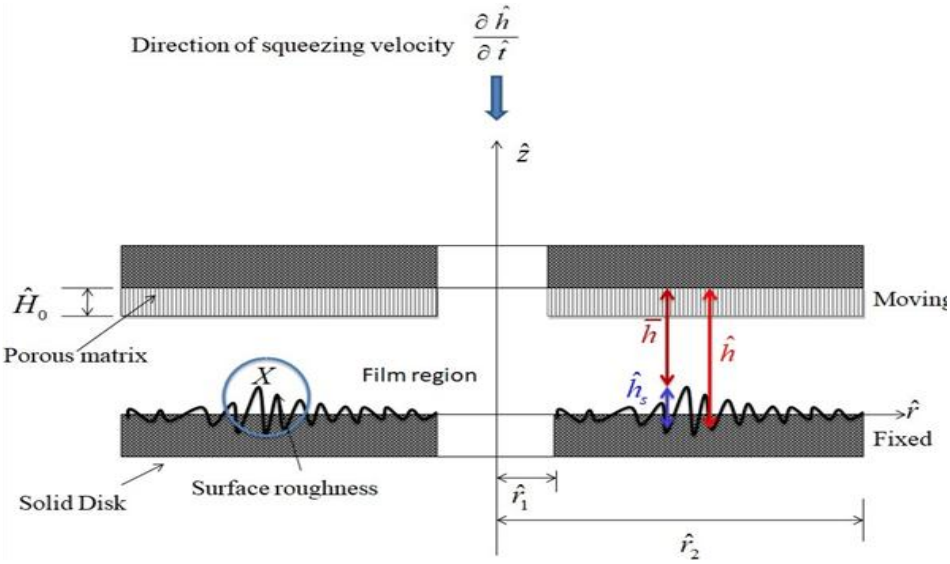

Figure: (A) Physicalcharacteristicsofasqueezefilmdesign

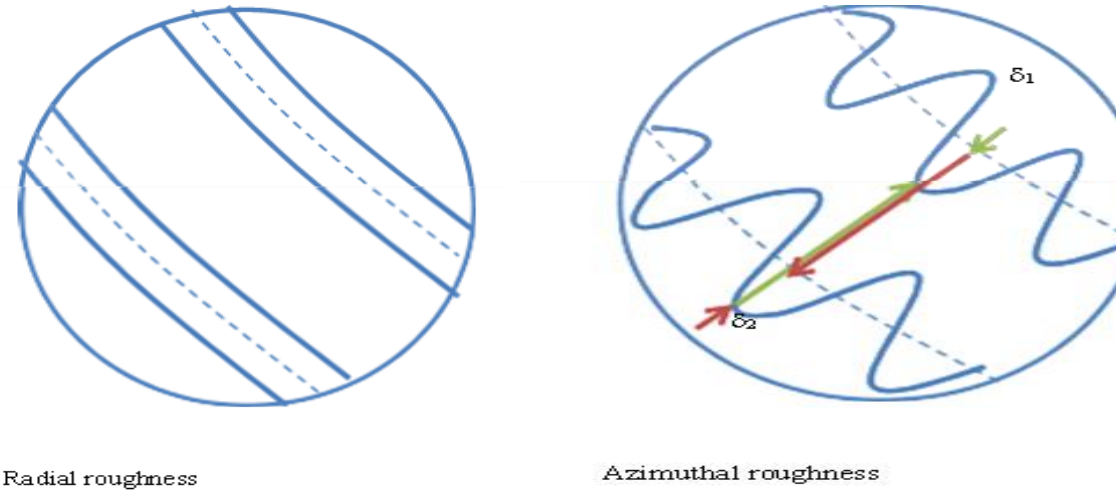

Figure: (B) Surfaceroughnessofporousroughannulardisks [SEMI-ANALYTICAL APPROACH-BASED STUDIES OF THE SQUEEZE FILM LUBRICATION BETWEEN ROUGH POROUS ANNULAR DISCS: RABINOWITZ FLUID MODEL, 2023, Amit Kumar Rahula, Manoj Kumar Singha, Ravi Tiwarib, SourabhPaulb, PentyalaSrinivasaRaoc, RohahnBiswasd, ActaPolytechnica 63(6):439–450]